ANTHROPOLOGY

First systematic assessment of dental growth and development in an archaic hominin (genus, *Homo*) from East Asia

Song Xing[1,2]*, Paul Tafforeau[3], Mackie O'Hara[4], Mario Modesto-Mata[5,6,7], Laura Martín-Francés[5,8], María Martinón-Torres[5,7], Limin Zhang[1], Lynne A. Schepartz[9], José María Bermúdez de Castro[5,7], Debbie Guatelli-Steinberg[4,10,11]

Several human dental traits typical of modern humans appear to be associated with the prolonged period of development that is a key human attribute. Understanding when, and in which early hominins, these dental traits first appeared is thus of strong interest. Using x-ray multiresolution synchrotron phase-contrast microtomography, we quantify dental growth and development in an archaic *Homo* juvenile from the Xujiayao site in northern China dating to 161,000–224,000 years or 104,000–125,000 years before present. Despite the archaic morphology of Xujiayao hominins, most aspects of dental development of this juvenile fall within modern human ranges (e.g., prolonged crown formation time and delayed first molar eruption). For its estimated age-at-death (6.5 years), its state of dental development is comparable to that of equivalently aged modern children. These findings suggest that several facets of modern human dental growth and development evolved in East Asia before the appearance of fully modern human morphology.

INTRODUCTION

Among extant primates, humans are uniquely derived in the prolonged period over which their physiological systems grow and develop (*1*). Through actual or virtual histology (synchrotron microtomography), it is possible to assess, with high precision, the growth and development of one physiological system in fossils: the dentition (*2–3*). Fossil teeth preserve a record of daily (short-period) as well as longer-period growth lines in their hard tissues that can be imaged nondestructively in fossil teeth with synchrotron microtomography (*3–6*). With this method, a recent study showed that *Australopithecus* and *Paranthropus* species were more variable in their developmental rates than previously realized (*6*), although none appear to evince the prolonged periods of dental growth and development that characterize modern humans (*2, 7*).

The ages at which fossil specimens of early *Homo* reach dental developmental stages, however, appear to be encompassed within the modern human range of variation, although they generally fall at the advanced end of that range (*8*). With respect to Neanderthals, a recent study of a single specimen suggests that they, too, were encompassed within modern human ranges of dental development (*9*). Yet, other studies suggest that some individual Neanderthal specimens may have been exceptionally advanced as compared to modern humans (*4–5*).

Overlapping in time with Neanderthals during the Middle to Late Pleistocene were diverse hominin forms, most of which have been attributed to one (or occasionally more than one) of these taxa/groups: *Homo erectus*, *Homo antecessor*, *Homo heidelbergensis*, archaic *Homo*, Denisovans, Neanderthals, and anatomically modern humans (*10*). During this time period, recent studies have documented diverse hominin forms in East Asia (*11–12*), with as yet unclear relationships to Neanderthals, Denisovans, and anatomically modern humans. These new archaic finds from China are complicating our understanding of human evolution during this period of time. Despite the surge in studies of dental development in Middle-Late Pleistocene *Homo* (*3, 5–6, 9, 13*), very little is known about the dental growth and development of East Asian *Homo* during this time period.

Here, we ask: How similar or different were multiple aspects of East Asian archaic hominin dental growth and development from those of contemporary Neanderthals and anatomically modern humans? The answer to this question provides a first glimpse into a developmental system at a time and place in human evolution that is poorly understood. The present study addresses this question by using propagation phase-contrast x-ray synchrotron microtomography (PPC-SRμCT) and laboratory microtomography (μCT) to assess various features of dental growth and development in the archaic *Homo* Xujiayao 1 specimen from China in comparison with other hominins and modern humans.

The Xujiayao site, located in the Nihewan Basin of northern China, produced abundant hominin and faunal fossils in the late 1970s (*14–15*). The hominin remains include a juvenile maxilla and unassociated mature and immature cranial material found in the upper cultural layers (*15*). Several chronometric analyses have been performed, with late Middle Pleistocene [161,000 to 224,000 years or 104,000 to 125,000 years before the present (B.P.)] (*16–17*). Thus, a minimum age of over 100 thousand years (ka) can be assumed, while the fossils may date to over 200 ka B.P.

The consensus of a series of recent studies identifies the Xujiayao hominins as archaic *Homo* with a complex mosaic of morphologies, including characteristics found in *H. erectus*, modern humans, and Neanderthals (*11–12*). The Xujiayao hominins display several ancestral features, including a thick cranial vault and strongly built cranium, as well as robust and large teeth (*12, 14–15*). Features derived toward a modern human condition include high and rounded temporal squama, simple occlusal and smooth buccal surfaces on the maxillary premolars, and a symmetrical P^3 crown outline with a strongly reduced lingual cusp (*12*). The bony labyrinth structure of Xujiayao 15 temporal falls within the range of variation of Neanderthals and differs from that of other members of the genus *Homo* (*11*). It has also recently been suggested, given the size of the crowns and roots of Xujiayao teeth, that they may be Denisovan (*18*).

Modern human dental development is characterized by the following suite of features: slow trajectory of enamel growth, compacted perikymata in the cervical half of the crown, prolonged crown formation time, and delayed achievement of developmental stages and molar eruption ages relative to other extant primates (*2, 7, 19–20*). This suite of traits has not been documented as a package in other fossil hominins apart from anatomically modern *Homo sapiens* (*3*). Given that a mosaic pattern of morphological traits has been described for the Xujiayao individuals, an in-depth analysis of the dental microstructures, growth rates, and patterns of development conducted here yields insight into the possibility of a similar mosaic pattern in its dental growth and development and establishes where this archaic juvenile dentition falls on the hominin developmental spectrum.

Specifically, this study systematically investigates the following aspects of Xujiayao dental development: (i) long-period line periodicity, (ii) perikymata number and distribution, (iii) crown formation time, (iv) initiation time, (v) root extension rate, (vi) stages of dental development in teeth relative to one another as well as the dental age relative to the age-at-death, and (vii) estimated age at first molar eruption. These aspects of dental growth and development have been well studied in other recent hominins and in modern humans [e.g., (*5, 6, 13, 19*)] and show different patterns of variation across hominin taxa. Definitions of these variables are given in data file S1.

RESULTS

The Xujiayao 1 left hemimaxilla (Fig. 1) preserves seven developing teeth. The permanent incisor (I^1), canine (C′), third premolar (P^3), fourth premolar (P^4), and first molar (M^1) have completed crowns and present variably developed roots. The second molar (M^2) has an incomplete crown, with the hypocone approaching completion. The first molar (M^1) is fully erupted into occlusion. The deciduous canine (dc) to deciduous second molar (dm^2) are also in occlusion, but only the dm^2 roots remain. More detailed information on the developing stages for each tooth is provided in the text of data file S1.
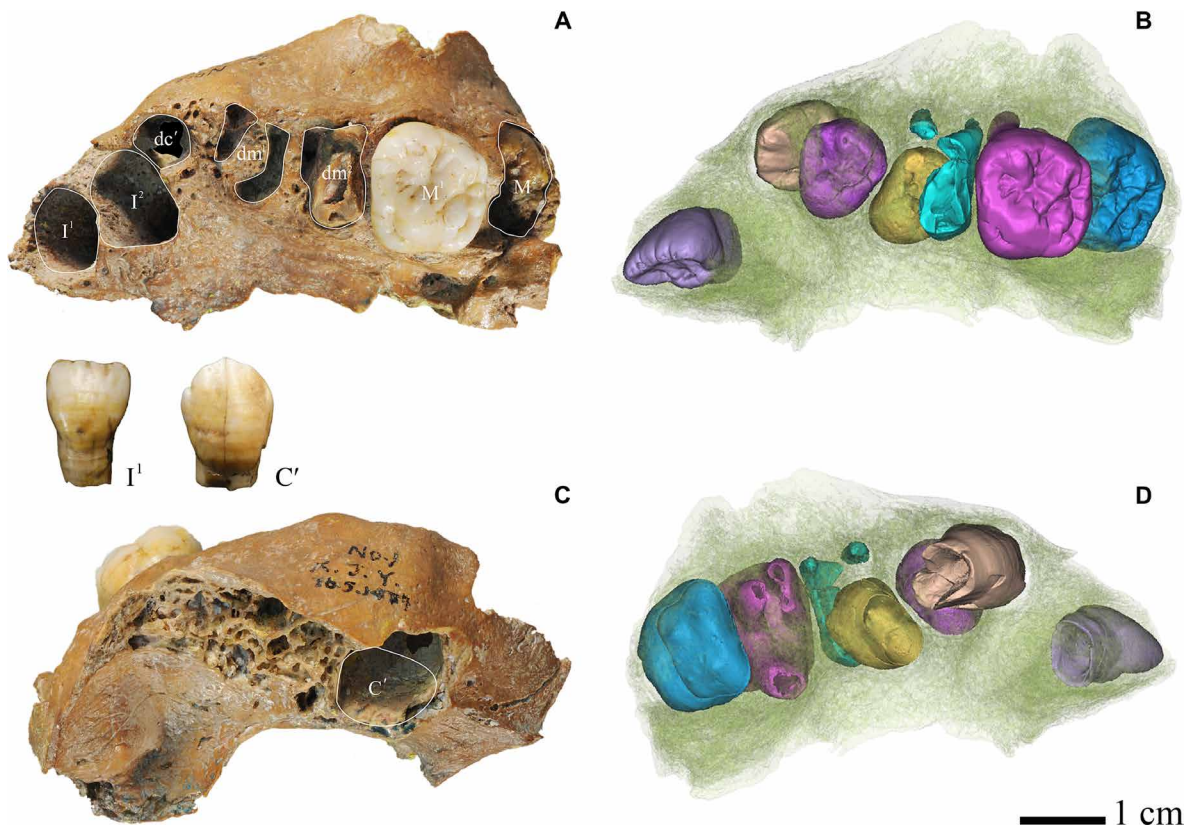

Fig. 1. Dental remains of the Xujiayao juvenile. Original Xujiayao fossil (A and C) and μCT reconstruction of all the teeth (B and D). M^1 and a part of the root of the deciduous dm^2 are visible in the superior view photo, as is the M^2 crown. I^1 and C were removed from their sockets and appear in the picture as isolated teeth. Note that P^3, P^4, and M^2 were still unerupted. (A and B) Inferior view. (C and D) Superior view. (A and C) Photographed by S.X. from Institute of Vertebrate Paleontology and Paleoanthropology, Chinese Academy of Sciences.

Long-period line periodicity

The PPC-SRμCT with submicrometer resolution of M^2 revealed a 10-day long-period line periodicity, which was applied for all of the teeth, as periodicity is the same across an individual's permanent teeth (fig. S1 and data file S2) [21].

Perikymata distribution

The percentage of perikymata in the cervical half of the crown is 60.8, 62.4, 65.6, 65.0, and 62.5% for I^1, C', P^3, P^4, and M^1, respectively.

Crown formation time

The crown formation times for I^1, C', P^3, P^4, M^1, and M^2 are 3.93 ± 0.10, 4.96 ± 0.04, 3.70 ± 0.13, 3.90 ± 0.14, 3.03 ± 0.01, and 3.61 ± 0.05 years, respectively (Table 1 and table S1).

Age-at-death

Here, we estimate the age-at-death by adding the postnatal enamel formation time of M^1 paracone cusp (where the neonatal line can be observed) (fig. S1) to the total lateral enamel formation time across teeth. The latter variable involves lateral enamel formation time estimated from four sections of perikymata (see Materials and Methods for more details) on M^1, C', P^4, and M^2. Estimated age-at-death was calculated to be 2377 ± 47 days or 6.51 ± 0.13 years. Estimation of average root extension rate and age at gingival emergence of the first molar was calculated, in part, on the basis of this age-at-death estimate.

Initiation time

By cross-matching linear enamel hypoplasia (LEH) (fig. S2 and data file S1), the initiation times for I^1, C', P^3, P^4, M^1, and M^2 were calculated to be 318 ± 35, 198 ± 14, 743 ± 37, 830 ± 1, −18, and 974 ± 54 days, respectively (Table 1 and Fig. 2). Thus, the full sequence of dental development was calculated (Fig. 2).

Average root extension rate

On the basis of the root length (fig. S2) and formation time (Table 1 and table S1), the average root extension rates for I^1, C', P^3, P^4, M^1, and M^2 are 11.06 ± 0.25, 8.19 ± 0.18, 7.41 ± 0.83, 8.25 ± 0.72, 9.74 ± 0.34, and 7.74 ± 1.43 μm/day, respectively.

Stages of dental development and dental ages

On the basis of the scoring system from Moorrees *et al.* [22] presented in Table 1, the dental age of the Xujiayao juvenile based on modern human standards for each tooth and the entire dentition were determined following the methods introduced by Shackelford *et al.* [23] (Table 2). The Xujiayao juvenile's age-at-death (6.51 ± 0.13 years) is within 2 SDs of the dental formation ages estimated for each tooth. The median attainment age (6.62 years) of the Xujiayao juvenile, predicted by considering all teeth together, is very close to its age-at-death as calculated from histological analysis (6.51 ± 0.13 years) (Table 2).

Estimated age at gingival emergence of the first molar

At death, the Xujiayao juvenile had its M^1 erupted into occlusion for a very short time based on the slight occlusal wear. The exact age at M^1 gingival emergence cannot be known. However, based on the number of months between gingival emergence and full eruption in chimpanzees and modern humans [20], the estimated M^1 emergence age is ~6.00 years of age.

DISCUSSION
Dental development characteristics and comparisons
Perikymata number and distribution

Perikymata number and distribution vary by tooth type and across Middle to Late Pleistocene hominin taxa [19]. Across all tooth types, Neanderthals average a smaller percentage of total perikymata in the cervical half of their teeth, although the range overlaps with modern humans (Fig. 3 and table S2). A description of the perikymata number and distribution for the Xujiayao I^1 and C were published previously [24] and will be referenced in this analysis. All the Xujiayao permanent teeth fall within the range of one or both of the modern human groups on the bivariate plots [Fig. 3; figure 2 of [24]]. The Xujiayao teeth almost always fall outside of the range of Neanderthals; the exceptions are P^3 and P^4, for which Xujiayao falls just within the Neanderthal range.

Overall, the Xujiayao juvenile exhibits a combination of total perikymata number and percent of perikymata in the cervical half of the tooth that is most similar to that of modern humans (and to

Table 1. Dental development data for the Xujiayao 1 juvenile. Periodicity = 10 days, based on M^2. Periodicity was determined from M^2 (mesiobuccal surface).

	Cusp		Crown		Root			Moorrees developmental stage
	Thickness (μm)	Formation time (days)	Initiation (days)	Total perikymata	Formation time (days)	Length (μm)	Average extension (μm/day)	Formation time (days)	
I^1	1350 ± 10	375 ± 2	318 ± 35	106 ± 4	1435 ± 38	6,893 ± 135*	11.06 ± 0.25*	624 ± 26	R1/2
C	883 ± 35	267 ± 9	198 ± 14	154/155	1812 ± 14	3,013 ± 450*	8.19 ± 0.18*	367 ± 47	R1/4
P^3†	1164 ± 26	334 ± 6	743 ± 37	101 ± 5	1349 ± 49	2,083 ± 23	7.41 ± 0.83	285 ± 35	Ri
P^4†	1361 ± 31	378 ± 7	830 ± 1	105 ± 5	1423 ± 52	1,028 ± 49	8.25 ± 0.72	125 ± 5	Ri
M^1‡	1082 ± 32	315 ± 7	−18	79 ± 1	1105 ± 3	12,546 ± 54	9.74 ± 0.34	1290 ± 50	R3/4
M^2‡	1270 ± 9	358 ± 2	974 ± 54§	96 ± 2§	1318 ± 18§	622 ± 72	7.74 ± 1.43	85 ± 25	Cr.c

*Root length and root extension rates are given after reconstruction of the broken parts.   †Measurements based on buccal cusp.   ‡Measurements based on mesiobuccal cusp.   §The perikymata number at the paracone apex area of M^2 cannot be precisely ascertained, and we provide a minimum estimate. All the values inside the parentheses are influenced by this.
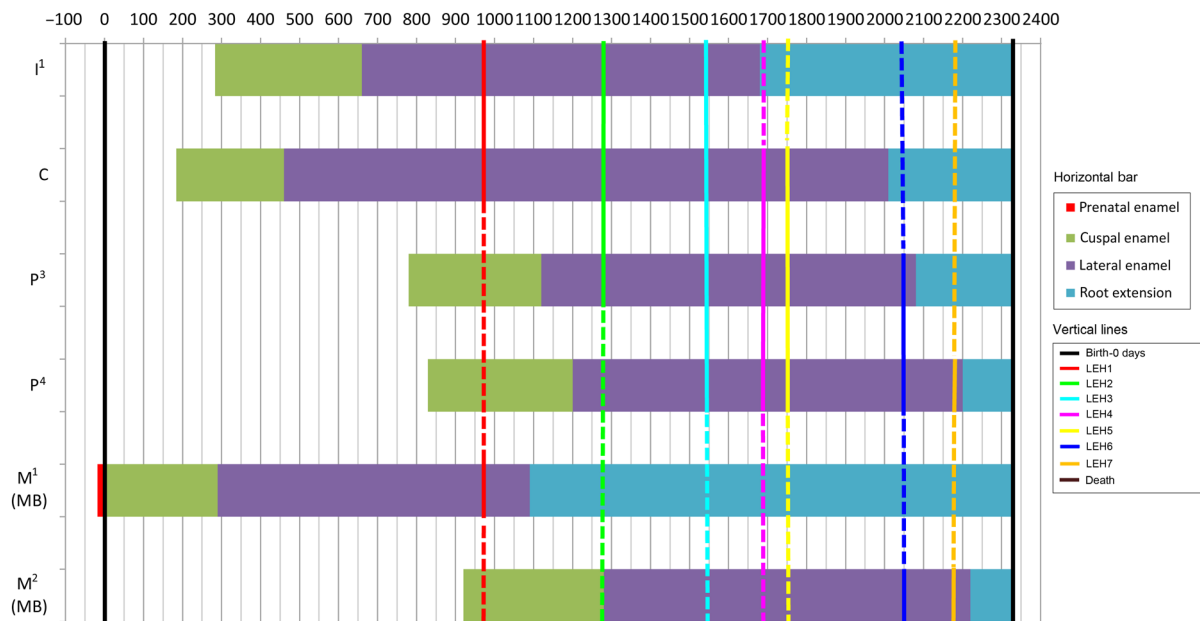
Fig. 2. Developmental chart of the Xujiayao permanent teeth. The vertical lines were dashed when the stress lines have not been detected in that portion of the tooth. MB, mesiobuccal cusp.

Table 2. Estimates for the Xujiayao 1 dental age (in years) based on modern human standards. The dental age of the Xujiayao juvenile was estimated on the basis of each tooth or all teeth following the methods introduced by Shackelford *et al.* (*23*), in which the graphical data of Moorrees *et al.* (*22*) were transformed into numerical parameters for deriving the median attainment ages of certain dental formation stages. In Moorrees *et al.* (*22*), 10 permanent tooth categories including 2 maxillary incisors and 8 mandibular teeth were used. The estimates for Xujiayao's dental age were based on the data for the maxillary I[1] and the mandibular P[3], P[4], M[1], and M[2] of modern humans.

	Stage	−2 SD	−1 SD	Median attainment age	+1 SD	+2 SD
I[1]	R1/2	5.74	6.46	7.25	8.12	9.10
C	R1/4	4.88	5.64	6.51	7.49	8.60
P[3]	Ri	4.90	5.52	6.19	6.95	7.78
P[4]	Ri	5.73	6.41	7.17	8.02	8.95
M[1]	R3/4	4.46	5.00	5.59	6.24	6.96
M[2]	Cr.c	5.26	5.90	6.61	7.39	8.26
All teeth	—	6.02	6.32	6.62	6.95	7.28

modern southern Africans in particular). The distribution of perikymata in living humans appears to be related to changes in rates of enamel extension along the enamel-dentine junction (EDJ) (*25*). It is possible that the Xujiayao individual's perikymata distribution pattern indicates a pattern of extension rate change more similar to that of living humans than to that of Neanderthals, although other enamel formation processes may be involved (*25*).

Crown formation time

To calculate the total crown formation time, both cuspal and lateral enamel formation time must be known. Cuspal enamel thickness is used to calculate cuspal enamel formation time and will be briefly compared here across hominin groups (table S3). Modern human groups usually have thicker enamel than Neanderthals but thinner enamel than Plio-Pleistocene hominins (*5–6*). Across all tooth types, except for C′ and M[2], the cuspal enamel of all the Xujiayao teeth is thicker than that of

Neanderthals. The Xujiayao C′, P[3], M[1], and M[2] fall within the range of modern human groups; the P[4] cuspal thickness measurements fall above the range of modern humans and closer to the fossil *H. sapiens* range. For I[1], the Xujiayao juvenile has much thicker cuspal enamel (1350 ± 10 μm) than all other hominins measured to date.

It has been suggested that first molar crown formation time, in particular, is related to the pace of life history across primates (*26*), although this is debated (*20*). On average, Neanderthals take longer to complete their crowns than do Plio-Pleistocene hominins but complete them in less time than do modern humans (table S4). When the ranges reported for southern African and Newcastle modern humans are combined, the Xujiayao juvenile falls within the combined modern human range for I[1] and P[3]. The crown formation time of the Xujiayao C′, P[4], M[1], and M[2] fall slightly above the combined range of recent modern humans (table S4).
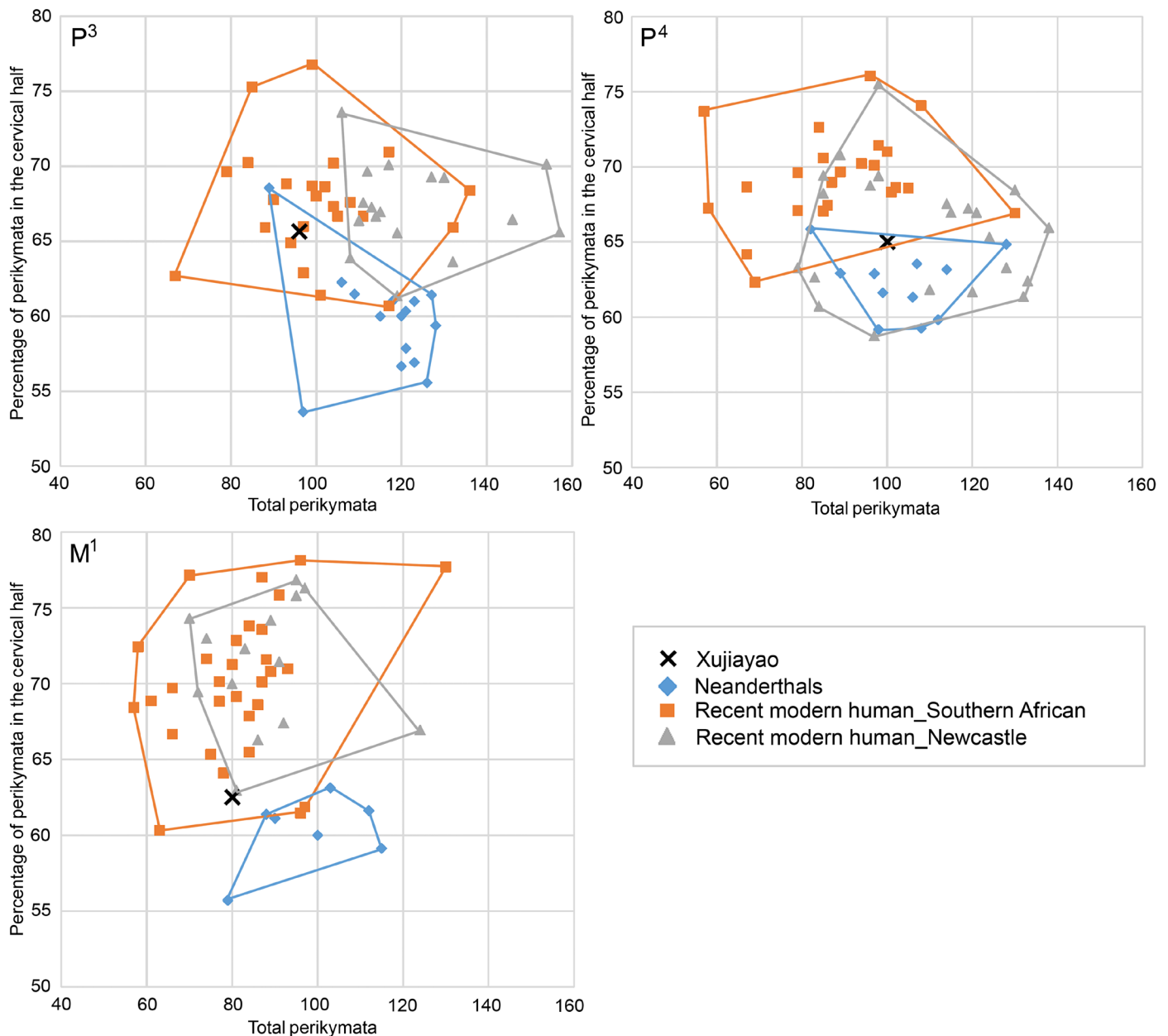
Fig. 3. Bivariate plots of percentage of perikymata in the cervical half of the crown versus total perikymata. This bivariate plots were prepared using the dataset from S.X., M.O., and D.G.-S. (table S2).

Initiation times

Other than M^1 that consistently starts mineralization around birth, the initiation times of permanent teeth exhibit a high degree of intra- and intertaxonomic variation (table S5). More data are needed to further explore taxonomic trends in initiation time.

The Xujiayao I^1 initiated at 318 ± 35 days of age, which is later than all available histological comparisons for modern humans and other hominins (and is closest to the 206 days of an early *Homo* specimen). The most marked result is that the canine initiated earlier than I^1. This is the first documented occurrence of this developmental phenomenon in fossil hominins. However, in modern human samples, canines initiating earlier than I^1 have been shown to occur (27). The initiation age of the other Xujiayao teeth all fall within or very close to the range of

variation for modern humans (table S5). In comparison to a *H. erectus* specimen from Sangiran (S7-37; 934 days), the Xujiayao P^4 initiated over 100 days earlier.

Root extension rate

Dean and Cole (28) showed that the pattern of extension rate change along the root, from the cemento-enamel junction to the root apex, differs distinctly between chimpanzees and modern humans. It is less clear what average root extension rates, as were calculated in this study, may reflect.

The Xujiayao I^1 root (reconstructed at 6.89 mm) grew at a rate of 11.06 µm/day, which is higher than that of recent modern humans [7.93 µm/day for the first 6.00 mm and 8.20 µm/day for the first 7.00 mm; see also (29)]. The M^1 root extended faster at 9.74 µm/day

than modern human roots of a similar size, which have an average extension rate of 6.28 μm/day [for the mandibular M_1; see (30)]. The Sangiran S7-37 maxillary M^1 root was reported to grow at a rate of 6.5 μm/day for its 11.40 mm length (8). The average root extension rate from one Neanderthal M_1 is 6.30 μm/day for its 13.3 mm length (13). The mandibular M_1 of Jebel Irhoud 3, a late Middle Pleistocene hominin from North Africa, has a 13.5-mm-long root and an extension rate of 9.60 μm/day (3), close to the value for the Xujiayao maxillary M^1.

Stages of dental development in teeth relative to one another and dental ages

Delayed development of anterior teeth relative to posterior teeth has been described as the "ape-like" pattern (31). However, there is substantial intraspecific variation in the relative development of anterior and posterior teeth. For example, in the fossil *H. sapiens* from Qafzeh, Qafzeh 10 had a delayed I^1 developmental stage (Ri) relative to its M^1 (R1/2), while Qafzeh 15 developed its I^1 and M^1 at a similar pace and approached the stage of R3/4 simultaneously (5). The Xujiayao I^1 is at stage R1/2, and M^1 is at stage R3/4. In a sample of 156 recent modern human children with M^1 at stage R3/4, 32.7% had I^1s at R1/2 (dataset shared by H. M. Liversidge), similar to what is observed for the Xujiayao juvenile.

In comparing the predicted dental development age with the calculated age-at-death for the Xujiayao juvenile, it appears that I^1 and P^4 formed at a slightly faster pace (~1.0-year difference) than the modal value for modern humans (Table 2). However, when within-tooth variation is considered [as per Shackelford *et al.* (23)], Xujiayao's histologically determined age-at-death (6.51 ± 0.13) is included within 2 SDs of the predicted dental ages for I^1, P^4, and M^2, as well as for other individual teeth. When both within-tooth and between-tooth variation (the whole dentition) are considered, the Xujiayao juvenile's age-at-death is very close to the median dental age estimated from modern human standards and falls within 1 SD of the median attainment age for modern humans (Table 2). These findings indicate that the Xujiayao juvenile dentition does not form at an accelerated schedule relative to that of modern humans. The large range of variation of dental ages estimated for each individual tooth of the Xujiayao juvenile (Table 2) suggests the need to be cautious when assessing dental age and/or age-at-death based on an isolated tooth versus the entire dentition.

Estimated age at M^1 emergence

The M^1 emergence age has been proposed to be highly concordant with life history events of great apes and modern humans, such as age at first reproduction and age at weaning (32–33). From Plio-Pleistocene hominins to modern humans, the eruption age of first molars gradually shifted to later ages, with most earlier hominins (both Plio-Pleistocene hominins and *H. erectus sensu lato*) (2, 20) being more ape-like in the M^1 emergence age [for *Pongo*; (33)] (table S6). The average age of gingival emergence for M^1 in modern populations from around the world varies from 5.1 to 7.0 years, while the range is 4.7 to 7.1 years for M_1 (34). The M^1 emergence ages of the Neanderthals Krapina 46 (Max B) and Devil's Tower 1, Gibraltar were estimated to be ~5.5 and ~5.1 years, respectively (5), while the La Chaise Neanderthal M1 was reported to have its gingival emergence at 6.7 years (13). The limited data for Neanderthals may suggest that their gingival emergence ages for first molars fall within the range of variation for modern humans.

With an estimated ~6.0 years of age for the M^1 gingival emergence, the Xujiayao juvenile erupted its first molar later than Plio-Pleistocene

hominins, *H. erectus sensu lato*, and comparably to most Neanderthals and modern humans.

The Xujiayao juveniles' combination of dental growth and development features in comparative context

At present, the earliest appearance of the various aspects of dental growth and development that characterize anatomically modern humans remains unclear (2, 5). When absolute timing and growth rates (i.e., crown formation time, first molar emergence, and rate of enamel formation) are considered, neither early *Homo* nor *H. erectus sensu lato* appear to exhibit the slow maturational mode of dental growth and development of modern humans (2, 6, 8). However, relative to Plio-Pleistocene non-*Homo* hominins, *H. erectus sensu lato* is shifted more toward the modern human condition (2). Dean and Liversidge (8) showed that the range of variation in dental development in modern humans is wide enough to accommodate early *Homo* and *H. erectus*, although these early members of the genus *Homo* fall at the advanced end of the modern human developmental spectrum.

For Neanderthal-lineage hominins (including *H. antecessor* and some European *H. heidelbergensis*), chronological data derived from histology on dental development are available only for Neanderthals themselves (3–5, 9, 13). The microstructures revealed by PPC-SRμCT indicate that most of Neanderthal teeth grow in shorter periods of time on average than those of *H. sapiens* (3–5). Although a recent study of the El Sidrón J1 Neanderthal demonstrates that its stage of dental developmental is encompassed well within modern human ranges (9), most Neanderthal individuals appear to lie within the advanced end of the modern human developmental spectrum, with some perhaps falling below it (5, 23). Neanderthal first molar eruption ages, however, fall within modern human ranges (5, 13). Comparison of perikymata distribution patterns among taxa reveal that relative to *H. sapiens*, Neanderthal-lineage hominins have a smaller percentage of their total perikymata packed into the cervical halves of their crowns (19). The Jebel Irhoud 3 juvenile, a late Middle Pleistocene hominin from North Africa and described as having early modern human affinities, was found to have prolonged crown formation times as well as stages of development, and eruption comparable to those of modern humans at similar ages, but with rapid rates of root extension (3). Thus, with the Jebel Irhoud 3 juvenile, which appears to be an early modern human, dental development and eruption are firmly within modern human ranges.

With the exception of fast rates of root extension, most aspects of dental growth and development in the Xujiayao juvenile are also well within modern human ranges (table S7). Xujiayao 1 has prolonged crown formation times and first molar eruption timing similar to that of modern humans. Xujiayao's stage of dental development is similar to that of comparably aged modern children. The perikymata distribution pattern that tends to separate modern humans from early *Homo* and Neanderthals (19, 24) also groups the Xujiayao juvenile with modern humans. Therefore, although the Xujiayao juvenile has a mosaic of morphological characteristics, retaining a combination of modern and archaic features, its rates of dental growth and development are generally encompassed comfortably within modern human ranges (with the exception of its rapid average rate of M^1 root extension and late I^1 initiation).

The Xujiayao dentition represents the earliest appearance in the fossil record of East Asia of dental development comparable to that of modern humans. Modern human life history is characterized by an exceptionally prolonged period of childhood dependency, delayed

ages at first reproduction, and long lifespans, i.e., modern humans "live slow and die old"(*1*). Investigations of human life history evolution have mainly depended on anatomical information retained in the fossil teeth of young juveniles [e.g., (*3–6*)]. In this context, the similarity of the Xujiayao juvenile to modern humans in its crown formation times, state of dental development, and estimated age at first molar eruption may suggest the presence of a slow life history comparable to that of modern humans.

MATERIALS AND METHODS
Comparative specimens
The present study compares the Xujiayao values for dental developmental variables to those of hominins reported in previous publications (see reference list in tables S2 to S6). In addition, we include previously published data for Neanderthals and modern humans from southern Africa and Newcastle (UK) [see (*19*)].

µCT and PPC-SRµCT scanning of Xujiayao teeth
The Xujiayao 1 maxilla was scanned by µCT for assessing developmental stages of all deciduous and permanent teeth (Fig. 1 and data file S1). All six permanent teeth were scanned with PPC-SRµCT on beamline ID19 of the European Synchrotron Radiation Facility (Grenoble, France) using a voxel size of 6.34 µm (data file S1). A 0.742-µm voxel size of PPC-SRµCT scanning was performed on the cuspal apex of the M^1 paracone to image the neonatal line (fig. S1), on the cuspal apex of the M^2 paracone for the enamel daily secretion rate (DSR), and on the lateral enamel of M^2 for long-period line periodicity (fig. S1 and data file S2). Thirty-micrometer-thick slices were generated in VGStudio 2.2 and VGStudio MAX 3.0 for the observation of periodicity and neonatal line. Two hundred–micrometer–thick slices were used in the measurement of enamel thickness and root length.

Regarding the relatively recent nature of the Xujiayao fossils, there may be a possibility of still having ancient DNA (aDNA) traces preserved. In order not to endanger any future aDNA analysis on this specimen, special care during the synchrotron experiment was taken to ensure that low-dose delivery was possible while still reaching sufficient data quality to perform the dental development analysis, following the recommendation of Immel *et al.* (*35*) and using the same dose quantification protocol and material.

Considering that the detection limit for effect of x-rays on aDNA is 200 Gy (water equivalent surface dose), we adapted the synchrotron scanning protocols for full teeth imaging to stay below this limit (about 150 Gy), keeping in mind that, up to 2000 Gy, the damage is negligible and would not endanger aDNA study. The dose given to the whole specimen during the conventional scan was not measured but can be estimated from the scanning parameters to be 1.4 Gy, i.e., without any detectable effect on aDNA (data file S1). Dose being cumulative, the complete scan history of the specimen has to be taken into account and recorded. Only the scans performed at submicrometer resolution resulted in accumulated dose above the detection limit, but on very restricted volumes each time (about 3.5 mm × 1.6 mm), and located mostly in enamel. In these areas, the total accumulated surface dose reached a maximum of about 5500 Gy (probably less due to beam attenuation by the sample itself), corresponding to a maximum aDNA loss of 20% [see (*35*) for more details]. Orientation of the teeth for submicrometer resolution scanning was optimized to reduce as much as possible the amount of material crossed by the beam during the scans, to ensure that only the scanned area

would receive an x-ray dose, potentially leading to some aDNA degradation.

Perikymata counting
Perikymata counting was carried out on the virtual three-dimensional models of the Xujiayao teeth, reconstructed from the 6.34-µm data PPC-SRµCT scanning using VGStudio 2.2 and VGStudio MAX 3.0. For each tooth, a series of eight views were generated all around the tooth for general perikymata assessments. Among these views, we observed the labial or buccal surfaces of I^1 and C', the buccal cusp of P^3, the buccal cusp of P^4, and the mesiobuccal cusp of M^1 and M^2, as well as the distolingual cusp of M^2. The interobserver error of perikymata counting varied from one to five (Table 1). For comparison to other hominins in total perikymata numbers and percent perikymata in the cervical region of the tooth, only one set of perikymata counts was used—the set calculated by S.X., M.O., and D.G.-S. It is this set that is most comparable to the comparative datasets in which D.G.-S. was involved.

Calculation of crown formation time
The crown formation time is calculated as the sum of the formation time of cuspal enamel and lateral enamel. Cuspal DSR is not constant during the whole cuspal enamel secretion, and it is often observed that the DSR increases when distance from EDJ increases, especially in thick-enameled taxa. It is also observed that, for different teeth of a single individual, the teeth having thinner enamel (such as anterior teeth) will exhibit cuspal DSR equivalent to the inner and middle values measured on the molars with thicker enamel, suggesting a general relationship between DSR and distance to the EDJ applying on the whole individual. Hence, instead of using a single value for DSR, we developed a method consisting of quantifying the gradient of DSR versus distance to the EDJ on M^2 of this individual. From this gradient, it becomes then easy to derive an equation relating the cuspal thickness with the cuspal formation time, applicable on all the teeth of this individual, taking into account that average DSR of thinner-enameled teeth would be lower than that of thicker-enameled ones. DSR was measured three times in three different sections to quantify the inner, middle, and outer DSR on the M^2 cuspal enamel of paracone (data file S1). For each measurement, a prism between two consecutive Retzius line was traced and its length was recorded in ImageJ. From these measurements, a simple regression was applied to relate the averaged measured DSR with their corresponding distance to the EDJ. It turned out that a simple linear regression was sufficient to efficiently characterize the DSR gradient in this individual (DSR = $0.00146 \times dis_{EDJ} + 2.70$; $R^2 = 0.812$). From this gradient, the general equation relating cuspal enamel thickness and cuspal formation time was derived by simulating the complete secretion profile from EDJ to 1770 µm (thickest cuspal enamel observed for this individual), leading to the following polynomial equation: $y = 1.20E{-}8x^3 - 7.99E{-}5x^2 + 0.363x + 0.556$, where y is the cuspal enamel formation time and x is the cuspal enamel thickness (data file S1). Cuspal enamel thickness was measured from the dentine horn to the first perikymata on the outer enamel surface. The cuspal enamel thickness of the other teeth was then put into this equation, and the secretion time of their cuspal enamel was calculated (data file S1). Even if this approach is somehow experimental, it can be expected to be more relevant than using a single average value to estimate cuspal formation time over a complete dentition exhibiting very different cuspal enamel thicknesses. Lateral enamel formation times were calculated by multiplying

the number of perikymata by the individual's periodicity (10 days). The interobserver error of crown formation time varies from 3 to 52 days, depending on slight differences in the measurement of cuspal enamel thickness and perikymata counts between observers (Table 1 and table S1).

Estimation of age-at-death

The age-at-death was estimated using two sets of data:

1) Post-natal cuspal enamel formation time in the paracone of M^1: Post-natal cuspal enamel formation time is equal to the cuspal enamel formation time minus prenatal enamel formation time. We first measured the cuspal enamel thickness of the M^1 paracone and then used the equation described in the previous section to obtain its formation time (see the previous section for more details of the equation). The cuspal enamel formation time of the M^1 paracone is 315 ± 7 days (Table 1). Then, we identified the neonatal line, which can be observed on both enamel and dentine in the M^1 paracone (fig. S1). The distance between the enamel neonatal line and dentine horn tip is measured as 48 μm, and therefore, the prenatal enamel formation time for M^1 is 18 days based on the equation presented above. Subtracting 18 days of prenatal enamel formation time from two different estimates of cuspal enamel formation time (315 ± 7 days) from the two sets of authors yields a postnatal cuspal enamel formation time estimate for the M^1 paracone of 297 ± 7 days.

2) Total lateral enamel formation time: The root surfaces of Xujiayao permanent teeth are poorly preserved, making the counting of periradicular bands imprecise, so it is impossible to obtain the age-at-death based on one tooth (e.g., M^1). Therefore, we cross-matched the first-formed M^1 paracone (buccal surface) until the last-formed M^2 hypocone (distolingual surface) perikymata through the buccal surfaces of C and P^4 using accentuated perikymata and LEH (fig. S2 and data file S1). The virtual reconstructions were used in the cross-matching, and they were obtained from synchrotron scanning at a resolution of 6.34 μm and μCT scanning at a resolution of 43.0 μm (data file S1). Because the crown of the M^2 hypocone had not yet completed its formation, only counts of perikymata were involved in calculating age-at-death (fig. S2). Note that Fig. 2 shows the development of the M^2 paracone (mesiobuccal cusp), not the hypocone (the distobuccal cusp). The total lateral enamel formation time across all teeth is 2080 ± 40 days, calculated as follows: (10 days × number of perikymata counted on the M^1 lateral enamel to LEH1) + (10 days × number of perikymata counted on C′ between LEH1 and LEH4) + (10 days × number of perikymata counted on P^4 between LEH4 and LEH6) + (10 days × number of perikymata counted on the M^2 hypocone between LEH6 and the end of enamel development). The error in total lateral enamel formation time derives from differences between the two sets of observers in their counts of perikymata.

The two sets of data postnatal cuspal enamel formation time and total lateral enamel formation time were added together to obtain the age-at-death: 2377 ± 47 days or 6.51 ± 0.13 years.

Calculation of initiation time

This group of values was based on the cross-matching of LEH and accentuated perikymata on all of the Xujiayao permanent teeth (fig. S2 and data file S1). The time spent for all teeth between birth and the same LEH (e.g., LEH1), composed of initiation time, cuspal enamel formation time, and lateral enamel formation time before the LEH is the same. The initiation time of M^1 is −18 days (see the previous

section for more details). Using the initiation of M^1 and the cross-matching of the LEH across the other teeth, the initiation time of all the other Xujiayao permanent teeth can be calculated. For example, by cross-matching I^1 against M^1 (having neonatal line) using LEH1, I^1's initiation time can be calculated to be 283 days = 308 days − 18 days (cuspal formation time of the M^1 paracone after birth) + 68 perikymata (first perikymata to LEH1 of the M^1 paracone) × 10 days − 377 days (cuspal enamel formation time of I^1) + 31 perikymata (first perikymata to LEH1 of I^1) × 10 days. In fig. S2, we did not provide the buccal view of the M^2 paracone to provide a whole profile of cross-matching using the estimation of age-at-death. However, we provided the perikymata number (77 lines) between the paracone apex and LEH6. By cross-matching P^4 and M^2 using LEH6, the initiation time of M^2 is calculated to be 920 days = 829 days (initiation time of P^4) + 371 days (cuspal enamel formation time of P^4) + 85 (first perikymata to LEH6 of P^4) × 10 days − 360 days (cuspal enamel formation time of the M^2 paracone) + 77 (first perikymata to LEH6 of the M^2 paracone) × 10 days. The interobserver error varies from 1 to 54 days (Table 1 and table S1), depending on the difference on measurement of cuspal enamel thickness and perikymata counting.

Root extension rate

The age-at-death minus initiation time and crown formation time for each tooth resulted in its root formation time. The root length of I^1 (buccal surface), C′ (buccal surface), P^3 (buccal surface), P^4 (buccal surface), M^1 (buccal surface of paracone), and M^2 (buccal surface of paracone) were measured on the sectional plane in ImageJ after reconstruction of the missing parts for I^1 and C′. The root length, divided by corresponding formation time, gave the average root extension rate. For example, the root formation time of the M^2's buccal surface of paracone was calculated by subtracting the tooth's initiation time, cuspal enamel formation time, and lateral enamel formation time from the known age-at-death (2330 − (920 + 360 + 940)) = 110 days (table S1). The root length is 694 μm. Therefore, the average root extension rate of the M^2's buccal surface of paracone is 6.31 μ/day. The interobserver error varies from 0.18 to 1.43 μm/day and come from the difference on measurement of cuspal enamel thickness and root length, as well as the perikymata counting (Table 1 and table S1).

Defining the stages of dental development

The teeth were scored for stage of dental development using Moorrees *et al.* (*22*). Ages for stages of dental development for the Xujiayao juvenile (Table 1) were assessed on the basis of modern radiographic standards (taking into account that radiographs of developing dentition typically appear as less advanced than the real stage of the teeth) and compared to the actual age-at-death. To assess dental age by modern human standards, the guidelines of Shackelford *et al.* (*23*) were followed, which incorporate data on two maxillary incisors and eight mandibular teeth from Moorrees *et al.* (*22*).

Estimation of gingival emergence

Gingival emergence of M^1 was estimated by subtracting the approximate time between gingival emergence and full eruption from the age-at-death because the tooth had only just come into occlusion. In modern humans, the time between gingival emergence and the end of eruption is between 4 and 5 months; in chimpanzees, it is closer to 4 months (*20*). Thus, the age of gingival emergence of the Xujiayao M^1 can be estimated by subtracting the eruption time from its age-at-death.

SUPPLEMENTARY MATERIALS

REFERENCES AND NOTES

1. B. A. Bogin, Evolutionary hypotheses for human childhood. *Am. J. Phys. Anthropol.* **104**, 63–89 (1997).
2. C. Dean, M. G. Leakey, D. Reid, F. Schrenk, G. T. Schwartz, C. Stringer, A. Walker, Growth processes in teeth distinguish modern humans from *Homo erectus* and earlier hominins. *Nature* **414**, 628–631 (2001).
3. T. M. Smith, P. Tafforeau, D. J. Reid, R. Grün, S. Eggins, M. Boutakiout, J.-J. Hublin, Earliest evidence of modern human life history in North African early *Homo sapiens*. *Proc. Natl. Acad. Sci. U.S.A.* **104**, 6128–6133 (2007).
4. T. M. Smith, M. Toussaint, D. J. Reid, A. J. Olejniczak, J.-J. Hublin, Rapid dental development in a Middle Paleolithic Belgian Neanderthal. *Proc. Natl. Acad. Sci. U.S.A.* **104**, 20220–20225 (2007).
5. T. M. Smith, P. Tafforeau, D. J. Reid, J. Pouech, V. Lazzari, J. P. Zermeno, D. Guatelli-Steinberg, A. J. Olejniczak, A. Hoffman, J. Radovčić, M. Makaremi, M. Toussaint, C. Stringer, J.-J. Hublin, Dental evidence for ontogenetic differences between modern humans and Neanderthals. *Proc. Natl. Acad. Sci. U.S.A.* **107**, 20923–20928 (2010).
6. T. M. Smith, P. Tafforeau, A. Le Cabec, A. Bonnin, A. Houssaye, J. Pouech, J. Moggi-Cecchi, F. Manthi, C. Ward, M. Makaremi, C. G. Menter, Dental ontogeny in Pliocene and early Pleistocene hominins. *PLOS ONE* **10**, e0118118 (2015).
7. T. G. Bromage, M. C. Dean, Re-evaluation of the age at death of immature fossil hominids. *Nature* **317**, 525–527 (1985).
8. M. C. Dean, H. M. Liversidge, Age estimation in fossil hominins: Comparing dental development in early *Homo* with modern humans. *Ann. Hum.Biol.* **42**, 415–429 (2015).
9. A. Rosas, L. Ríos, A. Estalrrich, H. Liversidge, A. García-Tabernero, R. Huguet, H. Cardoso, M. Bastir, C. Lalueza-Fox, M. de laRasilla, C. Dean, The growth pattern of Neandertals, reconstructed from a juvenile skeleton from El Sidrón (Spain). *Science* **357**, 1282–1287 (2017).
10. G. C. Conroy, H. Pontzer, *Reconstructing Human Origins: A Modern Synthesis* (W. W. Norton & Company, 2012).
11. X.-J. Wu, I. Crevecoeur, W. Liu, S. Xing, E. Trinkaus, Temporal labyrinths of eastern Eurasian Pleistocene humans. *Proc. Natl. Acad. Sci. U.S.A.* **111**, 10509–10513 (2014).
12. S. Xing, M. Martinón-Torres, J. M. Bermúdez de Castro, X. Wu, W. Liu, Hominin teeth from the early Late Pleistocene site of Xujiayao, Northern China. *Am. J. Phys. Anthropol.* **156**, 224–240 (2015).
13. R. Macchiarelli, L. Bondioli, A. Debénath, A. Mazurier, J.-F. Tournepiche, W. Birch, M. C. Dean, How Neanderthal molar teeth grew. *Nature* **444**, 748–751 (2006).
14. M. Wu, Human fossils discovered at Xujiayao site in 1977. *Vertebr. Palasiat.* **18**, 227–238 (1980).
15. L. P. Chia, Q. Wei, C. Li, Report on the excavation of Hsuchiayao man site in 1976. *Vertebr. Palasiat.* **17**, 277–293 (1979).
16. T. Chen, S. X. Yuan, S. Gao, The study on uranium-series dating of fossil bones as an absolute age sequence for the main Paleolithic sites of North China. *Acta Anthropol. Sinica* **3**, 259–269 (1984).
17. Z. Li, Q. Xu, S. Zhang, L. Hun, M. Li, F. Xie, F. Wang, L. Liu, Study on stratigraphic age, climate changes and environment background of Houjiayao Site in Nihewan Basin. *Quat. Int.* **349**, 42–48 (2014).
18. M. Martinón-Torres, X. Wu, J. M. Bermúdez de Castro, S. Xing, W. Liu, *Homo sapiens* in the eastern Asian Late Pleistocene. *Curr. Anthropol.* **58**, S434–S448 (2017).
19. D. Guatelli-Steinberg, D. J. Reid, Brief communication: The distribution of perikymata on Qafzeh anterior teeth. *Am. J. Phys. Anthropol.* **141**, 152–157 (2010).
20. J. Kelley, G. T. Schwartz, Life-history inference in the early hominins *Australopithecus* and *Paranthropus*. *Int. J. Primatol.* **33**, 1332–1363 (2012).
21. C. M. FitzGerald, Do enamel microstructures have regular time dependency? Conclusions from the literature and a large-scale study. *J. Hum. Evol.* **35**, 371–386 (1998).
22. C. F. A. Moorrees, E. A. Fanning, E. E. Hunt Jr., Age variation of formation stages for ten permanent teeth. *J. Dent. Res.* **42**, 1490–1502 (1963).
23. L. L. Shackelford, A. E. S. Harris, L. W. Konigsberg, Estimating the distribution of probable age-at-death from dental remains of immature human fossils. *Am. J. Phys. Anthropol.* **147**, 227–253 (2012).
24. S. Xing, D. Guatelli-Steinberg, M. O'Hara, X. Wu, W. Liu, D. J. Reid, Perikymata distribution in *Homo* with special reference to the Xujiayao juvenile. *Am. J. Phys. Anthropol.* **157**, 684–693 (2015).
25. D. Guatelli-Steinberg, B. A. Floyd, M. C. Dean, D. J. Reid, Enamel extension rate patterns in modern human teeth: Two approaches designed to establish an integrated comparative context for fossil primates. *J. Hum. Evol.* **63**, 475–486 (2012).
26. G. A. Macho, Primate molar crown formation times and life history evolution revisited. *Am. J. Primatol.* **55**, 189–201 (2001).
27. D. J. Reid, D. Guatelli-Steinberg, Updating histological data on crown initiation and crown completion ages in southern Africans. *Am. J. Phys. Anthropol.* **162**, 817–829 (2017).
28. M. C. Dean, T. J. Cole, Human life history evolution explains dissociation between the timing of tooth eruption and peak rates of root growth. *PLOS ONE* **8**, e54534 (2013).
29. M. C. Dean, P. Vesey, Preliminary observations on increasing root length during the eruptive phase of tooth development in modern humans and great apes. *J. Hum. Evol.* **54**, 258–271 (2008).
30. M. C. Dean, A radiographic and histological study of modern human lower first permanent molar root growth during the supraosseous eruptive phase. *J. Hum. Evol.* **53**, 635–646 (2007).
31. B. H. Smith, Patterns of dental development in *Homo, Australopithecus, Pan,* and *Gorilla. Am. J. Phys. Anthropol.* **94**, 307–325 (1994).
32. B. H. Smith, Life history and the evolution of human maturation. *Evol. Anthropol.* **1**, 134–142 (1992).
33. J. Kelley, G. T. Schwartz, Dental development and life history in living African and Asian apes. *Proc. Natl. Acad. Sci. U.S.A.* **107**, 1035–1040 (2010).
34. H. M. Liversidge, Variation in modern human dental development, in *Patterns of Growth and Development in the Genus Homo*, J. L. Thompson, G. E. Krovitz, A. J. Nelson, Eds. (Cambridge Univ. Press, 2003), pp. 73–113.
35. A. Immel, A. Le Cabec, M. Bonazzi, A. Herbig, H. Temming, V. J. Schuenemann, K. I. Bos, F. Langbein, K. Harvati, A. Bridault, G. Pion, M.-A. Julien, O. Krotova, N. J. Conard, S. C. Münzel, D. G. Drucker, B. Viola, J.-J. Hublin, P. Tafforeau, J. Krause, Effect of X-ray irradiation on ancient DNA in sub-fossil bones—Guidelines for safe X-ray imaging. *Sci. Rep.* **6**, 32966–32969 (2016).
36. D. J. Reid, M. C. Dean, Variation in modern human enamel formation times. *J. Hum. Evol.* **50**, 329–346 (2006).
37. D. J. Reid, A. D. Beynon, F. V. Ramirez Rozzi, Histological reconstruction of dental development in four individuals from a medieval site in Picardie, France. *J. Hum. Evol.* **35**, 463–477 (1998).
38. M. C. Dean, A. D. Beynon, D. J. Reid, D. K. Whittaker, A longitudinal study of tooth growth in a single individual based on long- and short-period incremental markings in dentine and enamel. *Int. J. Osteoarchaeol.* **3**, 249–264 (1993).
39. D. Antoine, "*Evaluating the periodicity of incremental structures in dental enamel as a means of studying growth in children from past human populations*," thesis, University College London, London, UK (2001).
40. P. Mahoney, J. J. Miszkiewicz, R. Pitfield, C. Deter, D. Guatelli-Steinberg, Enamel biorhythms of humans and great apes: The Havers-Halberg Oscillation hypothesis reconsidered. *J. Anat.* **230**, 272–281 (2016).

ScienceAdvances

First systematic assessment of dental growth and development in an archaic hominin (genus, *Homo*) from East Asia

Song Xing, Paul Tafforeau, Mackie O'Hara, Mario Modesto-Mata, Laura Martín-Francés, María Martinón-Torres, Limin Zhang, Lynne A. Schepartz, José María Bermúdez de Castro and Debbie Guatelli-Steinberg

ARTICLE TOOLS	http://advances.sciencemag.org/content/5/1/eaau0930
SUPPLEMENTARY MATERIALS	http://advances.sciencemag.org/content/suppl/2019/01/14/5.1.eaau0930.DC1
REFERENCES	This article cites 37 articles, 6 of which you can access for free http://advances.sciencemag.org/content/5/1/eaau0930#BIBL
PERMISSIONS	http://www.sciencemag.org/help/reprints-and-permissions

Use of this article is subject to the Terms of Service